134L Final Paper: Ground-based Visible Light Photometry of Supernova

June 2023

Supernovae, beyond being an interesting phenomenon in their own right, have been a powerful tool for probing the origin of the elements and the expansion of the universe. This paper will discuss how my partner and I used the Las Cumbres Observatory telescope network to probe the brightest supernova in recent years. I will discuss image processing techniques used, the limitations we came up against, and the data pipeline we created to turn our raw images into calibrated magnitude data.

1 Introduction

Supernovae are particularly exciting because they are transient: they are one of the few deep space objects where change can be easily observed over periods of time measured in days and weeks, rather than millions of years. They are also some of the brightest objects, outshining entire galaxies and giving us insight into parts of the universe far too distant to see any other single object. Although the last supernova in the Milky Way occurred 140 years ago, supernovae are readily observable by smaller ground-based telescopes such as LCO's 0.4m telescopes, and brighter ones in galaxies closer to the Milky Way can be seen by small recreational telescopes. One such supernova is 2023ixf, which was first detected in the well-known Pinwheel Galaxy on May 19, 2023. This was particularly lucky for us, as it was the brightest supernova in several years. We were able to gather data across the last several weeks of the course which gave us a light curve, giving us insight into the nature of this type II supernova.

Historically, supernovae have been classified into two main types: type I and type II. Type II are defined by the presence of Hydrogen emission lines in their spectra, while type I do not. Type 1a Study of the spectra and light curves of supernovae has led to further subclassification as well as a theory of the origins, and fates, of different types. Type Ia supernovae result from thermonuclear explosion of a small white dwarf star. White dwarfs are stars that have undergone the main sequence of Hydrogen and Helium fusion. What is left is a star of mostly carbon and oxygen which is too cold to produce any nuclear fusion, and supports itself from collapse only by electron degeneracy pressure. This is stable unless the electron degeneracy pressure is overcome; this can occur when a white dwarf absorbs mass from a sibling star. The increased weight increases pressure and temperature, and once critical temperature is reached runaway thermonuclear reaction burns carbon and oxygen in a matter of seconds, exploding a star and emitting light 5 billion times brighter than the sun.

Since the critical mass required to ignite a white dwarf is (usually) constant, they possess the same amount of fusible material upon ignition and hence explode with the same intensity. For decades, the "standard candle" method was the primary technique used to estimate the Hubble Constant, which determines how fast the universe expands. This technique assumes that type Ia supernovae reach peak absolute intensity that is constant, and therefore its magnitude as measured from earth can be used to measure its distance, and spectrometry data can be used to measure redshift, and therefore how fast the supernova is receding. These two data points taken on many supernovae gave us the first accurate measurement of how quickly space itself is expanding. Eventually, these measurements gave us the rate of expansion of the universe, which led to the postulation of the existence of dark energy. In recent years, increasingly precise measurements have informed us about the nature of dark energy, specifically in how pressure and energy density of dark energy is related.

Type II supernovae tell a completely different story of stellar evolution. These result from stars 8 to 50 times more massive than our sun, which can propagate fusion further into heavier elements. Nickel and iron accumulate at the core, but these elements do not themselves produce energy during fusion. A heavy core accumulates, supported by electron degeneracy pressure. Once the Chandrasekhar limit of 1.4 solar masses is reached, degeneracy pressure is overcome. The core rapidly collapses, and the outer shell of the star accelerates under gravity to almost a quarter the speed of light. The core is compressed to be extremely dense until neutron-neutron forces take over, rebounding the falling matter and sending a shockwave outward. The core gets hot enough to emit a quick burst of neutrinos, some of which are absorbed by the outer shell and cause the ultimate supernova explosion. The neutrino burst is also observable, and another factor that distinguishes type II supernova. The super-dense core either forms a neutron star or a black hole. Aspects of these supernovae are not fully understood, and studying their light curves and spectra can yield information on how they expel matter into the universe.

Type IIb supernovae are a subclass of Type II. They exhibit two distinct peaks in their light curve, likely caused by an outer layer of hydrogen and an inner core composed mostly of helium. As the outer shell is ejected outward, the Hydrogen absorbs less and less of the radiation from the exploding collapsed core. The duel peaks in magnitude indicate a complex interaction between inner and outer parts of the exploding star that is not completely understood.

Supernovae do not just emit a bright but short-lived flash of light into the universe; they affect

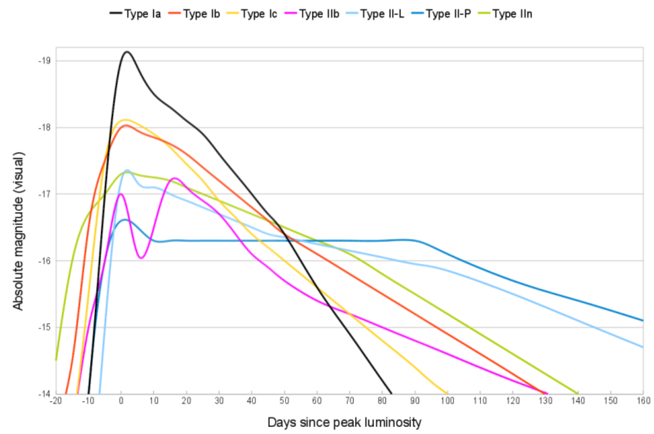

Figure 1: Light curves of various supernova types

many different areas of cosmology. They fling heavier elements into space, which can lead to formation of metal-rich stars which may be more likely to harbor planets. Their shockwave can destabilize nearby gas fields, yielding new stars; our own solar system may have formed due to a supernova. Their remnants, black holes and neutron stars, can produce measurable gravitational waves, and the nebula they leave behind can be some of the most beautiful objects observable in the night sky.

2 Collection Methods

Our initial plan was to do a rough spectrometry on three supernovae using SSDS u, g, i, and r filters. Because type II has such a strong peak around the first Balmer Series Hydrogen emission line (656 nm), we thought that we could capture a significantly higher magnitude in the r-band. We chose three bright supernovae from Rochester's Latest Supernovae database: a type Ia, type II, and an unclassified supernova (Table 2). These supernovae all had magnitudes measured within several weeks past around magnitude 15, making them feasible to measure with LCO's 0.4m telescopes. For each, we calculated the signal to noise ratio given the telescopes' internal parameters, known

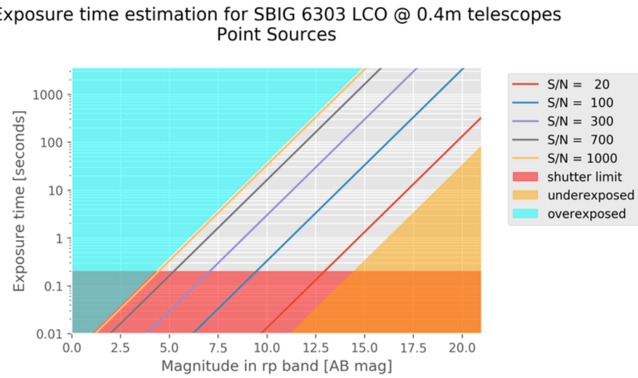

Figure 2: Light curves of various supernova types

magnitude, and exposure time. We observed how exposure time affected We aimed for an exposure short enough to avoid tracking issues and overexposure for reference stars, but long enough to capture a high signal to noise ratio in a single frame. This helped avoid stacking too many images, in which every image adds readout noise. Using the parameters in Table 2, signal to noise can be calculated as:

And the time needed to obtain a given ratio is:

$$S_N = S/N = FA_\epsilon\tau/[{N_R}^2 + \tau N_T]^{1/2}$$

and

$$\tau = \frac{{S_n}^2 N_T \pm \sqrt{{S_n}^4 {N_T}^2 + F^2 {A_\epsilon}^2 {S_N}^2 {N_R}^2}}{2F^2 A_\epsilon^2}$$

We also consulted Figure 2, which shows the non-linear relationship between exposure time and S/N ratio (note the logarithmic vertical scale). We settled on 250 seconds for u band and 100 seconds for the rest, which gave us a theoretical S/N ratio of roughly 30 - 60 across the board.

After viewing our first round of data, we realized that the u band was a waste of telescope time. Even though we requested a significantly longer exposure time for u-band and stacked multiple exposures, the signal to noise ratio was clearly not enough to yield meaningful results. For the supernovae, the u band did not capture a discernible light source at the location of any of our

Table 1: SNR Calculation Parameters, taken from LCO

Variable	**Description**	**Value Used**
F	Flux from the target	$310^6 10^{-\frac{2m}{5}}$
A	Telescope area	$\pi * 20^2$
τ	Integration time	?
ϵ	Telescope transfer efficiency	.5
Qe	Quantum efficiency	.3
NR	Readout noise	14.5
iDC	Dark Current	0.03
$F\beta$	Background flux	0.1
Ω	Angle of pixel	0.571

Table 2: Supernova Telescope Data Requests

Target Name	RA (J2000)	Dec (J2000)	Filter	Exposures per filter	Integration Time (s)	Accepted Magnitude	Accepted Type
AT2023gvj	14:55:34	-15:34:19	u, g, i, r	2	100, 100, 100, 250	15.4	unknown
2023gfo	13:09:40	-7:50:12	u, g, i, r	2	100, 100, 100, 250	15.3	II
2023foa	17:03:59	11:24:10.570	u, g, i, r	2	100, 100, 100, 250	15.2	Ia
2023ixf	14:03:39	54:18:41.940	i, r	25	15	10.9	IIL

Table 3: Astrophotography Telescope Data Requests

Target Name	RA (J2000)	Dec (J2000)	Filter	Exposures per filter	Integration Time (s)
Cat's Eye Nebula	17:58:33.42	66:37:59.52	u, g, r, i	10	75
M101	14:03:12	54:20:53:00	g, r, i	3	40

supernovae. For our first astrophotography project, the u-band picked up a blob at the center of the Cat's Eye Nebula, but it provided no definition that would add to the shape and color of the nebula. Overall, the sharp dropoff in light intensity reaching the earth's surface in the ultraviolet, caused mainly by absorption by ozone and the sun's black-body like spectrum which drops quickly below its peak wavelength, makes the u-band mostly useless for our purposes. We took this lesson forward and collected the rest of our data using only bands which have much higher signal to noise ratios for ground-based astronomy.

Half way through the quarter, we stumbled upon an Astronomy Picture of the Day depicting a newly discovered supernova in the relatively nearby pinwheel galaxy. Its magnitude was measured around 11, orders of magnitude brighter than the supernovae we were previously observing. Additionally, we caught it much earlier in its life than the previous events. We decided to capture a light curve for the rest of the time we had left. All images of ixf were captured in 15 second exposures to avoid overexposure. Our images were also offset from center so that the supernova and its host galaxy were in the bottom left. This was done to include more reference stars, which are generally scarce inside the area of bright galaxies like M101.

For our astrophotography project, we captured the Cat's Eye Nebula, a planetary nebula about 3000 light years away, due to its dynamic colors. Because the magnitude of the object is dispersed rather than a point source, we made a rough estimate of the right exposure time with the help of our LA Sam.

We decided to take another astrophotography of the Pinwheel Galaxy including the new IXF supernova. We increased the exposure time compared to our photometry data, allowing for some overexposure in order to capture the galaxy's finer structures. Having learned our lesson about u-band, we captured in i, g, and r filters only. The astrophotography telescope request data can be found in Table 3.

3 Data Analysis

3.1 Astrophotography

For the Cat's Eye Nebula, we stacked our exposures for each filter band, removing satellite streaks and aligning the exposures by stars. After realizing that u-band data was mostly useless, we decided to create a trichromy image using i band for red, r band for green, and g band for blue. Although these mappings do not provide an accurate depiction of what the nebula would look like to the naked eye, they give a visualization of light distribution over the light spectra. We got an interesting image with red (higher wavelengths) concentrated in the middle and green and blue (lower wavelengths) more in the fringes. Unfortunately we did not consider how small the solid angle of the nebula is compared to the field of view of our telescopes, and we did not get the resolution we were hoping for.

The i, r, g trichromy composite image of the pinwheel galaxy turned out significantly better. The higher solid angle yielded a higher resolution image of the object, and light from each band was more evenly detected throughout the galaxy. Galactic dust can be observed in red in the galaxy's spiral arms, and bright star clusters are seen in lower wavelengths. The supernova can be seen to the left and below the galaxy center, as the brightest point source in the longest spiral arm on the left side.

Figure 3: Light curves of various supernova types

Figure 4: Light curves of various supernova types

3.2 Data Processing Pipeline

For each set of images at a specific date and filter, we stacked them with star alignment, removing satellite streaks and skipping bad images when they occurred. Using AstroArt, we identified the supernovae by their right ascension and declination, adjusting white and black points to see if they were discernible. We then built a data pipeline in Python using AstroPy, AstroQuery, and other libraries. First, we adapted Sam Whitebook's photometry function to match our needs. We used AstroPy's DAOStarFinder, which scans for local maxima presumed to be stars, and records their position along with the sum of values within an aperture of radius 15 pixels. We converted pixel coordinates to R.A. and Dec. using AstroPy and the FITS header data. This photometry code is shown below.

Reference stars are found using AstroQuery from the SSDS database in a radius around the image. These positions are compared to star positions found in the image, and very close matches in the correct filter are logged as reference stars. The absolute magnitude from the reference stars present in our image, compared to their magnitudes from the database, were used to calculate a zero point for our image. This then lets us calculate the calibrated supernovae magnitudes using the flux equation. This calibration code, which also plots the image along with circles (red) marking detected stars, pink marking reference stars, and blue marking the supernova, are shown below.

$$M = -2.5 * \log(F) - Mag_{zp} \tag{1}$$

The flux equation, relating relative magnitude to the flux and the zero-point magnitude.

One key parameter which impacts the signal to noise ratio we capture using this pipeline is the

```python
def photometry(data, header, fwhm=5, thresh=5):
    sigma_clip = SigmaClip(sigma=3.0)
    bkg_estimator = MedianBackground()
    time = header["MJD-OBS"]
    mean, median, std = sigma_clipped_stats(data, sigma=3.0)
    bkg = Background2D(data, box_size=(50, 50), filter_size=(3, 3), sigma_clip=sigma_clip, bkg_estimator=bkg_estimator)
    bkg_median = bkg.background_median
    daofind = DAOStarFinder(fwhm=fwhm, threshold=thresh*std)
    sources = daofind(data - bkg_median)
    positions = np.transpose((sources['xcentroid'], sources['ycentroid']))
    apertures = CircularAperture(positions, r=15)
    phot_table = aperture_photometry(data - bkg_median, apertures)
    aperture_sums = phot_table['aperture_sum']
    posipos=np.where(aperture_sums>0)[0]
    astropycoords=[]
    wcs = WCS(header)
    positions=positions[posipos]
    aperture_sums=aperture_sums[posipos]
    for i in range(len(positions)):
      astropycoords.append(wcs.pixel_to_world(positions[i,0],positions[i,1]))
    return time, positions,aperture_sums ,astropycoords
```

Figure 5: Function that finds stars in image and calculates their flux

radius of the aperture used to capture star magnitude. In theory, this is a complex optimization problem which requires measuring the signal and noise in each pixel, modeling the S/N ratio per pixel as a curve that drops off from the center of the star, and finding the radius which optimizes the cumulative ratio. In practice, we looked at reference stars and our supernova, and found that for point sources that were not overexposed, a 15 pixel radius captured the brightest part of the star. LCO also states that for their 0.4m telescopes, a point source is smeared to a minimum 4-5 pixel full width, half maximum.

```
time, positions, aperture_sums,astropycoords=photometry(image, header, fwhm=5, thresh=7)
result = SDSS.query_crossid(astropycoords, photoobj_fields=['ra','dec','psfMag_'+filter_chosen,
                                                              'psfMagerr_'+filter_chosen],radius=5*u.arcsec)

ref_star_data=[]
for i in range(len(result)):
  if result['type'][i]=='STAR' and result['psfMag_'+filter_chosen][i]<16:
    ref_star_data.append(result[i])
ref_star_data=vstack(ref_star_data)

ref_star_locs=[]
ref_star_mags=[]
ref_star_err=[]
for i in range(len(ref_star_data)):
  ref_star_mags.append(ref_star_data['psfMag_'+filter_chosen][i])
  ref_star_err.append(ref_star_data['psfMagerr_'+filter_chosen][i])

  ref_star_locs.append(wcs.world_to_pixel(SkyCoord(ref_star_data['ra'][i],
                                                   ref_star_data['dec'][i], frame='icrs', unit='deg')))

ref_star_locs=np.array(ref_star_locs)
ref_star_mags=np.array(ref_star_mags)
ref_star_err=np.array(ref_star_err)


phot_x = positions[:,0]
phot_y = positions[:,1]
phot_flux = aperture_sums
calstar_flux = []
for j in range(len(ref_star_locs)):
    r = np.sqrt((phot_x - ref_star_locs[j][0])**2 + (phot_y - ref_star_locs[j][1])**2)
    index = np.where(r == np.min(r))[0][0]
    calstar_flux.append(phot_flux[index])

r = np.sqrt((phot_x - coords_pixels[0])**2 + (phot_y - coords_pixels[1])**2)
index = np.where(r == np.min(r))[0][0]
a=phot_flux[index]
roi_mag=-2.5*np.log10(a)

calstar_mag = -2.5*np.log10(calstar_flux)
```

Figure 6: Code to find reference stars and calibrate a zero point for the image, finding the ROI magnitude

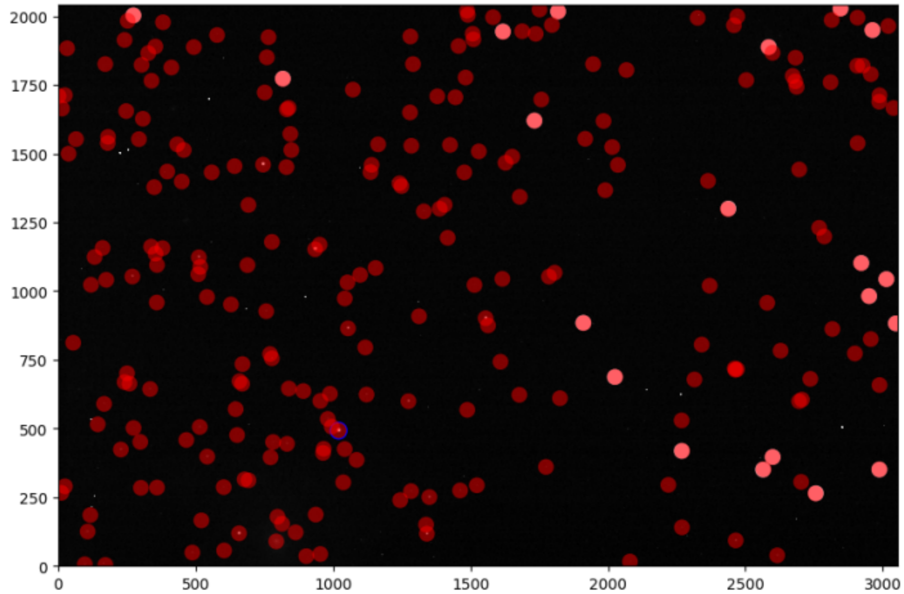

Figure 7: Example output for ixf, i band

3.3 Light curves

After obtaining calibrated magnitude data in each filter band for each of the six days collected from 5/24/23 to 6/11/23, we were able to plot a light curve. We found a distinct peak in both r and i band data at 6/04/23, with the r-band consistently brighter than the i-band. We corroborated our results with that of astronomer Yasuo Sano, and found peaks at similar times in both datasets. It is very likely that we captured the second peak of a type IIb supernova. Given that its initial discovery magnitude was very close to its initial peak, it is likely that this supernova peaked in magnitude around 5/20. Fifteen days later, we found another distinct peak, which can be explained by the type IIb classification. It is unlikely that we could have observed a distinct peak in any other type of supernova, due to the delay. This is exciting, all official sources have only reported the supernova as a type II so far.

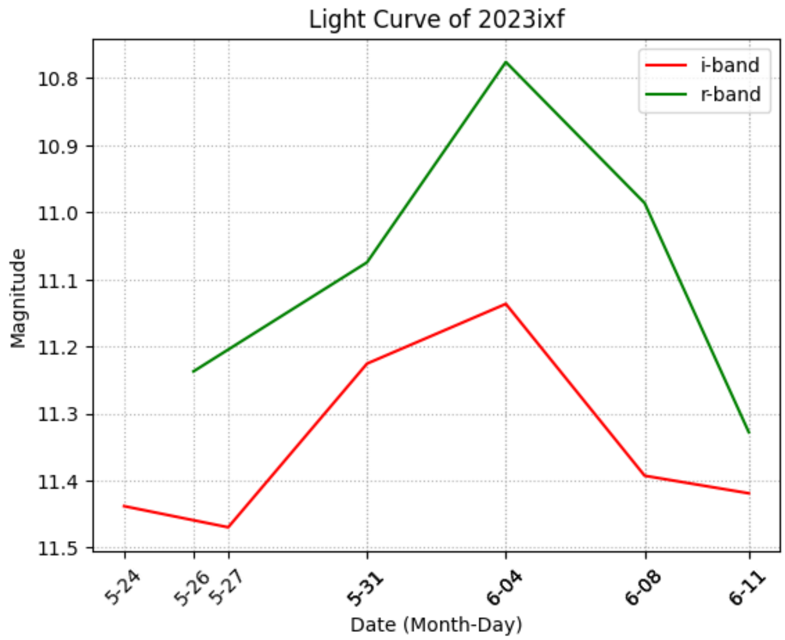

Figure 8: Our light curve, i and r band

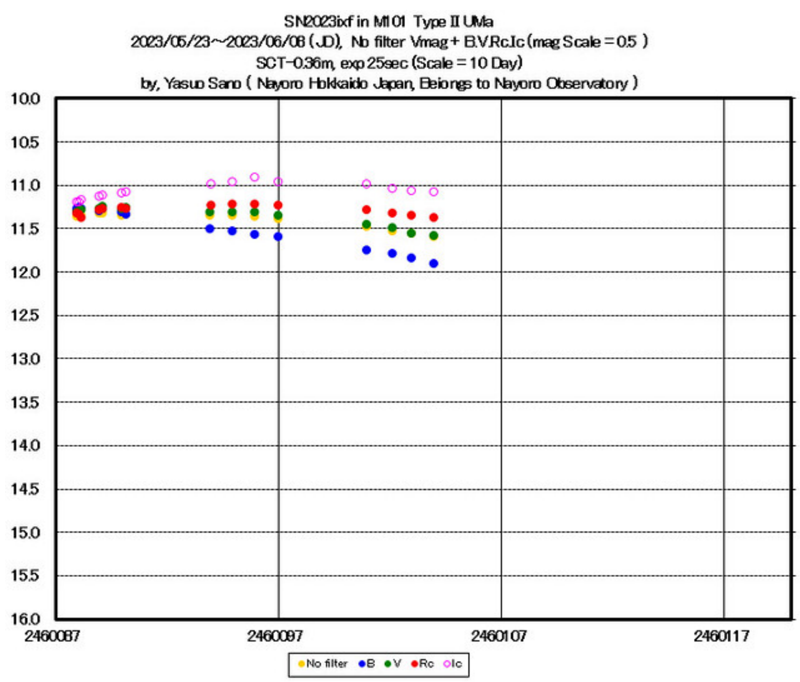

Figure 9: Reference light curve by Yasuo Sano

3.4 Spectral Data

Although we were not able to obtain spectral data directly, there is data available on the TNS database. This data seems to support our hypothesis for a type II-b supernova: The earliest data (5/19) exhibits Hydrogen emission lines, but the later (5/25) spectra looks more like a type Ia spectrum: no Hydrogen lines are present.

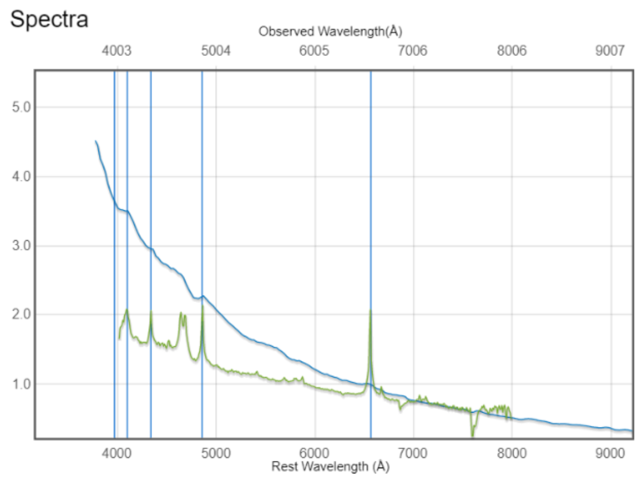

Figure 10: Spectral Data from 05/19 (Green) and 05/25 (Blue), taken from TNS

4 Discussion

4.1 Error analysis

In attempting to estimate error for our magnitude data, we saw two main sources, the signal to noise ratio which can be calculated from our images and the parameters of the telescopes used, and the error reported by the SSDS photometry database, which lists errors for the magnitude of each of the reference stars.

Because these sources of error come from independent sources and we assume magnitude measurements follow a Gaussian distribution, we could combine the errors by addition in quadrature. In practice, taking our relative error to be 2%, given that we aimed for a S/N ratio of 50, and propagating it through the magnitude-flux equation, our experimental error dwarfs the reported magnitude errors from the SSDS database reference stars. Overall, a magnitude delta of 0.1 is a reasonable rough estimate of uncertainty around the magnitudes we were measuring.

4.2 General Discussion

Our project, with a bit of cosmological luck, was able to successfully measure the evolution of a supernova as it peaked in intensity. The shape of the sup

A main factor holding us back from classifying supernovae by their type, and hence origin and fate, was that we lacked a spectrometer or narrow band filters from which we could discern the absorption spectra of Hydrogen and other elements. If we could do the project again with spectral data.

Getting better measurements of a type Ia supernova would have given us a real world example of how expansion of the universe is measured. If we found the peak magnitude of a Ia rather than type II supernova, we could have used it to estimate its distance by taking its absolute magnitude as a constant. If we had spectral data, we could have assumed its red shifted spectral peak as a constant, and used measured redshift to find its speed. From these two datapoints, we could generate our own rate of expansion and compare it to known data.

We also could have benefited from more time to do a light curve. Type II supernovae peak over several weeks and fade across many months. Although we successfully measured the supernova's peak, it would have been interesting to see how the longer light curve conformed to the pattern distinct to type II

Our project just covered one aspect of observation of supernovae. A future frontier for supernovae observation is neutrino detection. These particles are so light and interact with ordinary matter so little they are very hard to detect, but recent years have seen success in detecting small amounts. Neutrinos act as an "early warning" for type II supernovae: they penetrate out from the inner collapsed core before the entire star ignites. Knowing when a supernova is coming could help us point high resolution telescopes at it sooner, get a more detailed look at its earliest evolution.

5 References

Goobar, A., Leibundgut, B. (2011). Supernova cosmology: legacy and future. The Astrophysical Journal Supplement Series, 195(2), 34. https://doi.org/10.1088/0067-0049/195/2/34

Murphey, C. T., Hogan, J. W., Fields, B. D., Narayan, G. (2021). Witnessing History: Rates and Detectability of Naked-Eye Milky-Way Supernovae. The Astrophysical Journal Supplement Series, 253(2), 35. https://doi.org/10.3847/1538-4365/abdf6b

Scholberg, K. 2012, Supernova Neutrino Detection, Department of Physics, Duke University, Durham NC 27708, USA

Cameron, A. G. W., Truran, J. W. 1977, The Supernova Trigger for Formation of the Solar System, Icarus, 30, 447

Branch, D., Wheeler, J. C. 2017, Supernova Explosions, Astronomy and Astrophysics Library (Berlin: Springer)